

# Biochar nanoparticles: interactions with and impacts on soil and water microorganisms

Dwi C. Pratiwi<sup>1,2</sup>, Kurt O. Konhauser<sup>1</sup> and Daniel S. Alessi<sup>1</sup>

<sup>1</sup>Department of Earth and Atmospheric Sciences, University of Alberta, Edmonton, AB, Canada, <sup>2</sup>Fisheries and Marine Science Faculty, Universitas Brawijaya, Malang, East Java, Indonesia

## 12.1 Introduction

Biochar is the product of pyrolysis or carbonization of biomass (plant and animal) in the form of stable carbon-rich substances (Ahmad et al., 2014). Paz-Ferreiro et al. (2014) define biochar as an organic, low-density, carbonaceous product obtained from the pyrolysis of organic materials under limited oxygen conditions, where coproduced biogas and bio-oils can be used for energy. The low oxygen conditions are necessary to transform it into a charcoal-like product versus complete combustion to carbon dioxide. This leads to the formation of a solid carbon-rich residue named “char” (Kalus et al., 2019). Biochar surface properties control its stability and can influence solution chemistry including pH, chemical composition, and concentrations of ionic species (Chen et al., 2017; Liu et al., 2018). Particles of biochar range widely in size, from the nanometer to the centimeter scale, and 4.3% to 6.5% of the mass of biochar is present as colloids (Wang et al., 2013a,b). Following biochar production, biochar colloids inherent to the pyrolyzed material or generated in situ via physical or microbiological decay can be released into porewater and groundwater when biochar is applied to soils (Chen et al., 2017). The resulting colloids generally have lower aromaticity and a lower zeta potential than that of the corresponding bulk biochar (Safari et al., 2019; Yang et al., 2020a,b). In both soil and aquifers, BC has a strong affinity toward a range of heavy metals and organic contaminants (Zhang et al., 2010; Yang et al., 2019). Functional groups containing O and H have high electron affinities (for example, carboxyl and hydroxyl groups), and these negatively charged sites provide the sorption site for metal(loid)s and charged organic compounds, and can lead to the aggregation of biochar nanoparticles (BCNPs) with other colloids such as clays and microbes. As is discussed below, the zeta potential—an indicator of colloidal dispersion or aggregation—is strongly related to the biochar feedstock and pyrolysis conditions (Song et al., 2019).

While bulk biochar can act as a sorbent to immobilize potentially hazardous contaminants, BCNPs, the most common colloidal fraction, may function as a mode of transport of pollutants in the environment as they move with surface water or when they move through the subsurface as water in the vadose zone or groundwater. According to (Xu et al., 2017) particle sizes of between 1 nm to 1  $\mu\text{m}$  are considered dissolved black carbon and this fraction can be used to estimate the fate and transport of BCNPs in soil. Ultimately the mobility of BCNPs depends on the characteristics of the solution; for example, BCNPs aggregate more strongly in solutions containing divalent cations than in those dominated by monovalent solutions. For example, experiments have shown that at  $\text{pH} < 6$ ,  $\text{Na}^+$  and  $\text{Mg}^{2+}$  have less impact on the aggregation stability of BCNPs than have  $\text{Ca}^{2+}$  and  $\text{Ba}^{2+}$ . In addition, the biomass feedstock and the pyrolysis conditions used to produce a BCNP strongly influence subsequent particle aggregation in aqueous solution (Liu et al., 2018). Biomass contains cellulose, hemicellulose, and lignin. The decomposition of these components during the pyrolysis process results in a wide range of biochar compositions (see Section 12.2.1), and the resulting bulk biochar and the BCNPs have differing yields, physicochemical properties, and aggregation behaviors.

The presence of BCNPs has been reported to have toxicity effects on plants, animals (Nyoka et al., 2018) and microorganisms (Guo et al., 2019) at a level of risk comparable to engineered nanomaterials. For this reason, the rise in

biochar applications for the removal of metals and organic contaminants from water, for contaminant immobilization in soils, or for enhancing crop growth may also pose risks by introducing BCNPs to organisms present in aquatic ecosystems. A molecular-level understanding of these interactions is essential to describing how BCNPs impact organisms, if at all, during soil applications and remediation processes (Safari et al., 2019). In addition, electron transfer among organic contaminants, BCNPs, and microbial cells, can facilitate the degradation of organic contaminants (Fang et al., 2015a,b; Yu et al., 2015). During these interactions, the presence of BCNPs catalyzes the formation of persistent free radicals (PFRs) in the environment and can trigger microbes to generate reactive oxygen species (ROS) that may be toxic to certain members of soil and water microbial communities (Fang et al., 2015a,b). The interactions among contaminants, BCNPs, and microbes in the environment are outlined in (Fig. 12.1).

Agricultural plants may also feel the impact of BCNPs. Recent studies conducted by Zhang et al. (2020) investigated the impacts of BCNPs on seed germination and seedling growth of rice, tomato, and reed. The BCNPs feedstocks (rice straw and wood sawdust) were pyrolyzed at temperatures of 300°C, 500°C, and 700°C. The results show that for the rice experiments, all BCNPs types significantly extended the length of roots and shoots but inhibited the seed germination of rice. However, reed plants exposed to BCNPs collected from high-temperature biochar and lignin-rich feedstocks had dramatically decreased shoot lengths and plant biomass. There was no evidence that BCNPs impact the seed germination and seedling growth of tomato plants. Thus impacts of BCNPs on plants are variable depending on plant type and the nature of the BCNPs present in the rhizome.

The interactions between BCNPs and microbes continue to be studied, and comprehensive studies are required to provide systematic knowledge about the impacts of BCNPs to microbes in soil and water environments. Nevertheless, a study of the application of synthetic magnetite (Fe<sub>3</sub>O<sub>4</sub>)-biochar nanocomposites combined with photosynthetic bacteria (PSB) (*Rhodobacter capsulatus*) for wastewater treatment (He et al., 2016) found that when *R. capsulatus* was loaded onto the composites, the nutrients removal capacity of artificial wastewater (COD, NH<sub>4</sub><sup>+</sup>, PO<sub>4</sub><sup>3-</sup>) was considerably enhanced ( $p < 0.05$ ). The artificial wastewater, which contained glucose, NH<sub>4</sub>Cl, KH<sub>2</sub>PO<sub>4</sub>, MgSO<sub>4</sub> · 7H<sub>2</sub>O, NaHCO<sub>3</sub>, and CaCl<sub>2</sub> · 2H<sub>2</sub>O, showed removal of as much as 83.1% of the chemical oxygen demand (COD), 87.5% of the NH<sub>4</sub><sup>+</sup>, and 92.1% of the PO<sub>4</sub><sup>3-</sup>. The combination of PSB and BCNPs in this study proved an excellent agent for water treatment. Chen et al. (2012) conducted a longer-term incubation study (90 days) to observe the impacts of *Pseudomonas putida* exposed to BCNPs produced from wood chip (WC), bamboo leaf (BL), orange peel (OP), and pine needle (PN), pyrolyzed at 100°C, 300°C, 400°C, and 700°C and sieved to 0.154 mm. The effectiveness of the mixtures in biodegrading polycyclic aromatic hydrocarbons (PAH) in contaminated soil was investigated. The results show that microorganisms bound to BCNPs, according to the immobilized-microorganism technique (IMT), enhance the bioremediation of PAH-contaminated soil. After 28 days of incubation, PAH concentrations decreased by 21% (3-ring), 20% (4-ring), 25% (5-ring), and 32% (6-ring) relative to the blank control group (soil amended with sterilized water). The corresponding decreases were 11% (3-ring), 9% (4-ring), 12% (5-ring), and 27% (6-ring) higher than the control group (without

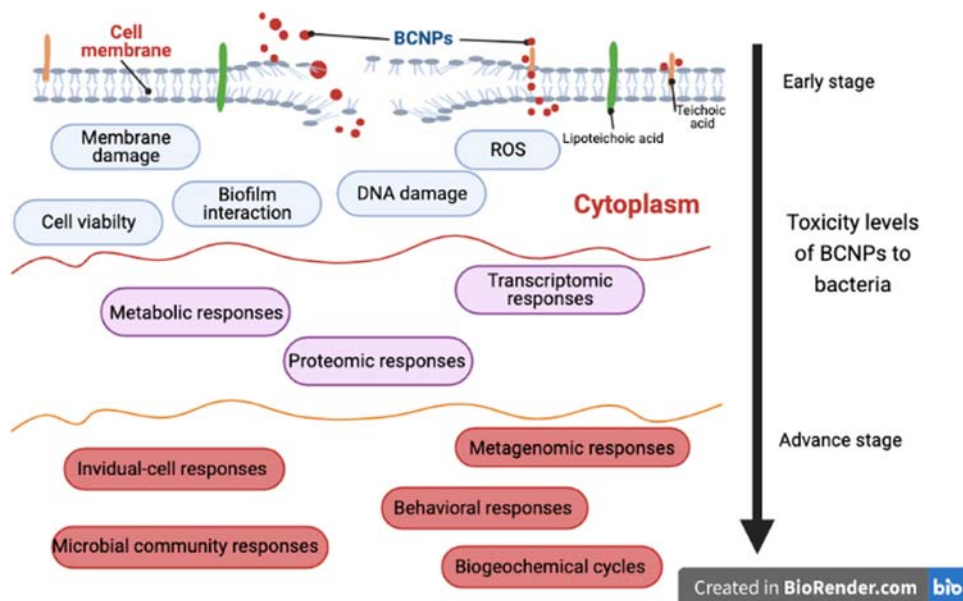


**FIGURE 12.1** Interactions between biochar nanoparticles (BCNPs) and contaminants and bacteria in the environment. Created in BioRender.com.

bacteria and BCNP). After 90 days of incubation, the PAH concentration decreased by an additional 6%–9% (3-ring), 6%–10% (4-ring), 7%–19% (5-ring), and 9%–29% (6-ring) as compared to the group without BCNPs.

The treatment of contaminated water with combined BCNPs and microbes or redox-active minerals may prove a promising new remediation approach. However, understanding how BCNPs loaded with potentially toxic trace metal (loid)s impact microbial growth, metabolism, reproduction, and toxicity during the water remediation process is a considerable research gap. It is important to address this gap to accurately predict the potential risks and environmental consequences of biochar field applications. Nevertheless, BCNPs utilization poses some advantages for agricultural soil decontamination and enhancement in plant growth. Therefore along with physicochemical properties-related factors, in this chapter, we will also discuss the applications of BCNPs in soil and water treatment, with a particular focus on BCNP-microbial cell interactions to build a comprehensive understanding of the potential impacts of BCNPs.

## 12.2 Generation of biochar nanoparticles

This section develops a comprehensive understanding of the production (feedstock and pyrolysis methods) of biochar to tailor the physicochemical properties of BCNPs which ultimately impact their transport and fate in the environment (Fig. 12.2).

### 12.2.1 Biochar properties

#### 12.2.1.1 Biomass

Waste biomass is a primary source material for the production of biochar, and its physical characteristics affect the properties of biochar. There are three common organic compound types in biomass: cellulose, hemicellulose, and lignin. These components are uniquely affected during pyrolysis of biomass and thus the product yield and physicochemical properties of the resulting biochar are different for each. Cellulose is a type of polysaccharide with no branching, and has a greater thermal stability compared to what hemicellulose and lignin have, decomposing at temperatures between 280°C–400°C (Weber and Quicker, 2018). Next comes hemicellulose which is a group of branched-chain molecules containing structures of polysaccharides. Of the three compound types in biomass, hemicellulose is the most active component during pyrolysis and decomposes at relatively low temperatures between 220°C–315°C (Yang et al., 2007).

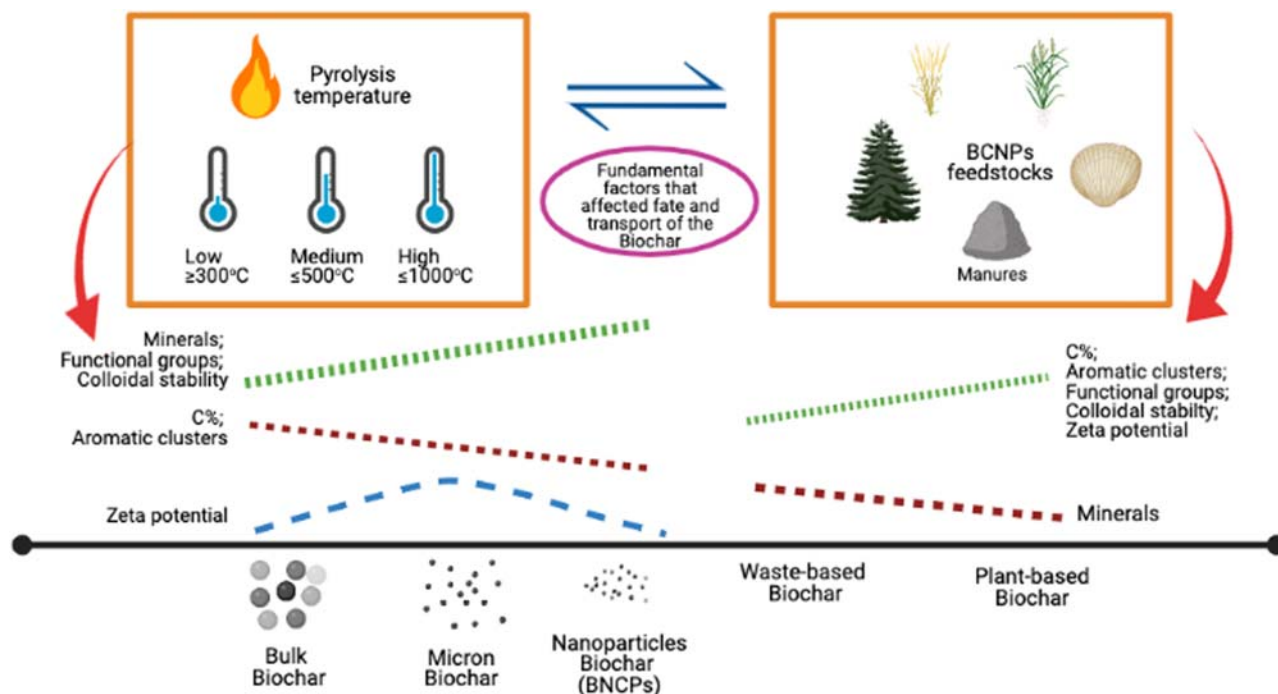


**FIGURE 12.2** Comparison of BCNPs production techniques and the impacts of resulting physicochemical properties on their transport and fate. Created in Biorender.com.

To degrade hemicellulose in biomass, torrefaction is the primary process used. Last, lignin is a complex three-dimensional macromolecule comprised of a variety of chemical bond types. For this reason, unlike hemicellulose and cellulose, lignin decomposes at a temperature hovering over a broader range of temperatures. Initial thermal degradation begins at 200°C and may require temperatures as high as 900°C to go to completion (depending on the residence time). Hence, special consideration must be given to the relative contributions of cellulose, hemicellulose, and lignin in biomass, which is critical to engineer the production of biochar with tailored physicochemical properties. Feedstock biomass for the production of biochar can come from various groups of organic raw materials. However, the most applicable and studied of feedstock resources are wood, herbs, and wastes (agricultural, animal manure, and sludge). Table 12.1 shows a comparison of physicochemical properties of BCNPs from various types of feedstocks.

In terms of BCNPs yield in the major biomass types, barley grass samples, a type of herb, had the greatest yield of BCNPs. By contrast, the woody sample produced the fewest nanoparticles, but ones that had the highest C mass fraction. Overall, the pyrolysis of plant biomass results in BCNPs that have higher concentrations of condensed aromatic rings and functional groups than those produced from wastes such as manure and sludge, which contain more ash. Furthermore, the higher minerals content in manure and sludge biochars, such as carbonates, phosphates, and silicates, prevents the condensation of carbon during pyrolysis. Similar to bulk biochar, oxygen- and hydrogen-containing functional groups in BCNPs impact their affinity for aqueous chemical species in the surrounding environment. However, in many low salinity freshwater environments, other forms of colloidal carbon, clays, microbes, and BCNPs have a net negative surface charge, causing repulsion and an enhancement in BCNP transport. Along with the feedstock biomass, pyrolysis conditions greatly impact the physicochemical properties of BCNPs, as is discussed in the following section.

### 12.2.1.2 Pyrolysis

Prior research has noted significant changes in structural complexity of biomass during pyrolysis for biochar production (Downie et al., 2012). The primary pyrolysis step produces light gases (such as CO, CO<sub>2</sub>, H<sub>2</sub>O, H<sub>2</sub>, and CH<sub>4</sub>), char, mineral ash, and tar. Char is the solid by-product of biochar production after the light gases and tar have been released from the pyrolyzed material. Tar obtained from slow pyrolysis is a complex substance comprising a diverse range of organic components such as aromatics hydrocarbon, aliphatic compounds, and oxygenated compounds (Downie et al., 2012). Unlike the loss of carbon during the formation of char, mineral ash and associated metal(loid)s remain after the pyrolysis and typically have low carbon content. Thus similar to the fixed carbon content, ash production increases with increased pyrolysis temperature. The main components of biomass ash include SiO<sub>2</sub>, CaO, K<sub>2</sub>O, P<sub>2</sub>O<sub>5</sub>, Al<sub>2</sub>O<sub>3</sub>, MgO, Fe<sub>2</sub>O<sub>3</sub>, SO<sub>3</sub>, Na<sub>2</sub>O, and TiO<sub>2</sub> (Vassilev et al., 2013). This ash can be a source of nutrients during soil application, and can also adsorb or induce the precipitation of metals in aqueous solution.

**TABLE 12.1** BCNPs properties from various feedstock (Song et al., 2019).

Feedstock	Sample <sup>a</sup>	Yield <sup>b</sup>	Ash	pH	C	H	O <sup>c</sup>	H/C	O/C
Wood	WC	1.12	43.4	8.90	17.7	3.01	39	2.05	1.66
	PW	0.99	32.6	9.40	44.9	3.40	19.1	0.91	0.32
Herbs	WS	9.60	65.5	9.69	6.57	1.75	22.2	3.20	2.54
	BG	15.3	67.3	9.17	5.02	1.49	24.8	3.56	3.71
Agricultural waste	PS	3.34	61.3	9.82	13.1	2.39	21.9	2.18	1.25
	RH	2.20	68.2	10.2	16.0	3.60	12.2	2.71	0.58
Animal manures	DM	6.74	56.6	9.76	6.58	1.77	32.0	3.23	3.65
	PM	4.60	68.5	9.22	4.21	2.47	21.9	7.04	3.89
Sewage	SS	1.42	60.8	8.43	11.2	3.47	21.6	3.72	1.45

<sup>a</sup>PW, pine wood biochar; WC, wood chip biochar; BG, barley grass biochar; WS, wheat straw biochar; PS, peanut shell biochar; RH, rice husk biochar; DM, dairy manure biochar; PM, pig manure biochar; SS, sewage sludge biochar.

<sup>b</sup>Yield (%) =  $M(\text{nano BC}) / M(\text{biochar}) * 100$ .

<sup>c</sup>O-content was calculated from C, H, and N content.

Pyrolysis temperature is a critical control parameter on biochar properties; increased pyrolysis temperature during biochar production decreased both H/C and O/C ratios (Weber and Quicker, 2018). Thus as pyrolysis progresses, the resulting biochar carbon content increases as the result of the separation of functional groups containing oxygen and hydrogen. The initial pyrolysis process starts with the drying of biomass. As the biomass is further heated, volatile matter is released from the solid. During pyrolysis the properties of the resulting biochar are controlled by factors including the heating rate, the highest temperature achieved during pyrolysis, reactor pressure, the residence time, properties of the reaction vessel (including orientation, dimensions, stirring, and the presence of a catalyst), pretreatment (e.g., drying, chemical activation), the flow rate of additional inputs (e.g., the use and fluxes of carbon dioxide, nitrogen, air, steam), and posttreatment (e.g., crushing, sieving, activation), if any. Lower temperatures yield biochars that are more functionalized, which are generally better for removing charged species from the aqueous solution (metals, for example). Higher temperatures yield more hydrophobic biochars that are often more efficient in removing organic contaminants from water (Paz-Ferreiro et al., 2014; Jin et al., 2016; Song et al., 2019; Yue et al., 2019).

During application of biochar to soils, it may impact the soil and the water chemistry, including pH, buffering capacity, nutrient content, and water retention. Several studies have reported the complex structures present in biochar, which are generated by processes including melting, fusion, or sintering and plastic deformation. The surface area and porosity of biochar is affected by the highest thermal temperature (HTT) achieved, high heating rates, increased pressure, long retention times (in consort with high temperature), and high ash-content (or low ash melting points). In addition, high pyrolysis temperatures result in increased surface area and porosity, yet reduce the density of functional groups at the biochar surface (Zhao et al., 2017; Jouhara et al., 2018; Leng et al., 2021). When applied for water retention in soils, biochars produced at high pyrolysis temperature, which have higher porosity and surface area but lower hydrophilicity, retain less water than do biochars produced from the same biomass at lower temperatures (Suliman et al., 2017).

During the carbonization process, there is thermal decay of the biomass structure. This results in a new configuration of the functional groups and the removal of oxygen and hydrogen. Biochars with lower H/C ratios contain more aromatic structures and lower concentrations of functional groups (Conti et al., 2014). Biochar with higher densities of aromatic structures is more suitable for soil amendment or metallurgical applications as it has greater stability. During pyrolysis, randomly organized aromatic rings form an amorphous phase. Following it, they condense to create polyaromatic sheets that comprise a crystalline phase that lends biochar its aromatic structure after production (McBeath et al., 2011).

The structure, concentrations, and types of functional groups impact the alkalinity of biochar, and ultimately it is the potential to neutralize acids that counts. Carbon content is among the most significant factors determined by the pyrolysis temperature and the composition of the initial biomass. These factors affect the alkalinity of biochar products because the higher the pyrolysis temperature is it leads to driving off more carbonates as CO<sub>2</sub>, resulting in a more acidic biochar. The carbonate content of the biomass produced at high temperatures is the major source of alkalinity (Yuan et al., 2011). Information on biochar alkalinity and its ash composition is vital prior to its application, for instance, to soils where the soil pH may need to be augmented to immobilize contaminants or promote crop growth.

Pyrolysis of plant biomass produces CO primarily, followed by CO<sub>2</sub>, CH<sub>4</sub>, and H<sub>2</sub> (Fu et al., 2011; Varma and Mondal, 2018; Amini et al., 2019). The gas present during pyrolysis profoundly impacts the surface properties of biochar. The use of CO<sub>2</sub> in the pyrolysis of biomass results in biochar with greater surface area and pore volume than one produced using N<sub>2</sub>. For example, an experiment conducted using oak-wood-derived biochar resulted in 463.6 m<sup>2</sup>/g of surface area and 106.5 cm<sup>3</sup>/g of pore volume when CO<sub>2</sub> was used, which is nearly twice of that when the same material was pyrolyzed in an N<sub>2</sub> environment (231.2 m<sup>2</sup>/g and 53 cm<sup>3</sup>/g, respectively) (Kim et al., 2019).

The energy content of biochar (per unit mass) increases with pyrolysis temperature (Weber and Quicker, 2018). Energy content increases most rapidly at pyrolysis temperatures ranging from 250°C to 350°C where most volatiles are generated. But beyond 400°C, the remaining charred material is relatively stable and shifts in energy content are small. Furthermore, carbon content is key to the use of biochar for specific applications. For instance, the use of biochar in the metallurgical sector requires very high fixed carbon content, hovering in the ranges of more than 90%–95%, which requires pyrolysis temperatures of 700°C or higher. The surface area and porosity of a particular biochar, along with the reactive surface functional groups on those surfaces, control its properties such as ion exchange capacity, water holding capacity and, ultimately, the contaminant retention properties of a particular biochar (Weber and Quicker, 2018).

Broader application of the biochar, and the amounts and types of BCNPs generated, depend on the final product characteristics. However, in terms of maximum porosity and surface area of the biochar product, the use of woody (lignocellulosic) feedstock, containing more lignin, and a moderate pyrolysis temperature (400°C–700°C) have been recommended (Yang et al., 2020a,b). In the next section, we discuss biochar production conditions impact the generation of BCNPs, and, ultimately, influence the applications of biochar for purposes including carbon sequestration, water treatment, and soil amendment.

### 12.2.1.3 Fate and transport of BCNPs

BCNPs have been applied as a sorbent for metal(oids) and organic compounds removal because their surface chemistry promotes contaminant sorption. The yield of BCNPs from bulk biochar varies, and is controlled by the source of feedstock and pyrolysis temperature (Wang et al., 2013a,b). Although BCNPs inherit the fundamental carbon component from bulk biochar, they show significant differences in physicochemical properties. For example, BCNPs contain less carbon and fewer aromatic structures, but have significantly higher mineral content, O-containing functional groups and colloidal stability, and zeta potential than what bulk biochar shows. In both soils and aquifers, BCNPs have a strong affinity toward a range of heavy metals and organic contaminants, and may be either attracted to or repulsed from soil minerals depending on the charge difference. Distinguishing factors such as these can make BCNPs highly reactive in soil and aqueous environments (Zhang et al., 2010; Song et al., 2019; Yang, et al., 2020a,b).

Song et al. (2019) reported a comparison of two of the feedstock sources of BCNPs production: plant waste biochar and municipal waste biochar. Plant waste BCNPs have significantly higher C content, functional group densities, aromatic structures, zeta-potential, and colloidal stability, and yet have lower minerals content than municipal waste BCNPs. The chemical differences between the two materials (Table 12.1) indicate that plant waste BCNPs have a stronger affinity for contaminants because metal(oid)s are primarily bound at aromatic groups containing oxygen-bearing functional groups. Contrarily, BCNPs derived from municipal waste have abundant carbonates, phosphates, and aluminosilicate minerals, which lead metals to complex and coprecipitate with this fraction instead of complexing and coprecipitating with the carbonaceous fraction.

The active mobility of BCNPs in certain soils can drive them vertically in soil profiles with infiltration and ultimately into groundwater systems (Hale et al., 2012; Oleszczuk et al., 2016). Thus contaminants sorbed to BCNPs, including organic compounds (Cao and Harris, 2010), inorganic compounds (Chen et al., 2008), antibiotics (Xing et al., 2016), and pathogenic microorganisms (Hale et al., 2012) can be transported from the site of the bulk biochar application, enhancing the dissemination of sorbed contaminants through colloid-mediated transport (Fang et al., 2015a,b). As discussed above, both the chemical and physical properties of the surrounding environment (ionic strength, pH, geologic medium, and presence of natural organic matter) and essential characteristics of the BCNPs (particle size distribution, composition, and surface chemistry) are essential factors in controlling their transport and fate.

The transport behavior of BCNPs in aqueous systems differs from that in the soils (Wang et al., 2010). The complexity and spatial variability of natural soil properties, including pH, the ionic strength (IS) of porewater, heterogeneity in the surface chemistry of soil particles, surface roughness, particle size distribution, and the presence of organic matter may influence BCNPs transport (Jaisi and Elimelech, 2009; Sagee et al., 2012; Wang et al., 2013a,b). Thus care should be taken when using bulk biochar or BCNPs for contaminant removal, as either can mobilize contaminants in the soil and the groundwater.

## 12.2.2 Biochar nanoparticles in the environment

BCNPs may have direct and indirect impacts on indigenous organisms within the habitat, ultimately affecting the mobility and speciation of nutrients, metals, and other contaminants. However, study of the properties of BCNPs and their impacts on organisms in soils and aquifers remain inadequate. Therefore the impacts on the environment of the application of BCNPs for environmental management are unclear and may be substantially different from the impacts of the application of bulk biochar. In this section, a description of how BCNPs can be used in various applications will be discussed to compare their function and performance.

### 12.2.2.1 Soil amendment

Biochar application for soil amendment widely suggests improved soil quality, plant diversity, and land-carrying capacity following application (Woods et al., 2009). However, BCNPs may reduce soil nutrition and pose potential risks to groundwater as BCNPs drive minerals downward in the soil profile (Hale et al., 2012). As discussed above, BCNPs often have higher densities of O-containing functional groups and minerals than has bulk biochar (e.g., Safari et al., 2019). Moreover, the colloidal stability of BCNPs increases with reduced particle sizes and IS, and is impacted by pH, which means the acidic and neutral conditions in water result in greater BCNPs stability than BCNPs would have in alkaline conditions (Song et al., 2019). Chen et al. (2012) investigated the transport and retention of BCNPs produced from WC in paddy soil under a variety of conditions. A WC feedstock was pyrolyzed under a nitrogen atmosphere at 500°C with a heating rate of 20°C/min. WC were selected as a feedstock because it yields relatively low mineral content in the resulting biochar, which minimizes potential disturbance to soil minerals upon amendment. The WC BCNPs were roughly spherical, with an average size of  $4 \pm 1.5$  nm. The experiment compared the behavior of BCNPs in

different soil conditions such as IS, electrolyte type (NaCl and CaCl<sub>2</sub>), and natural organic matter (0–10 mg/L humic acid). The initial IS experiments injected a solution containing 200 mg/L BCNPs, 50 mM NaCl and 1.0 mM CaCl<sub>2</sub> for 20 pore volumes (PV) into paddy soil columns. Following this, the columns were then eluted with another 10 PVs of 10 mM NaCl or 0.50 mM CaCl<sub>2</sub> with the hypothesis that lower IS would lead to the release of previously retained BCNPs. The results show that BCNP transport is inhibited at higher IS, irrespective of cation type (Ca vs Na). At increased concentrations of NaCl (1.0–50 mM) and CaCl<sub>2</sub> (0.1–1.0 mM), the mass recovery of BCNPs decreased from 44.8% to 12.3% and from 49.2% to 20.9%, respectively. The transport of WC biochar in paddy soil is significant, but considering that most natural soil contains fewer cations, the mobility of BCNPs is possibly greater in average soils. By contrast, in soils with abundant divalent cations, such as Ca<sup>2+</sup> in limestone rich regions, BCNPs may be retained, resulting in greater carbon enrichment and nutrient retention in those soil profiles than is possible in soils rich in monovalent ions (e.g., Na<sup>+</sup>). Finally, the greater mobility of BCNPs in the presence of HA, such as the paddy soil, suggests that BCNPs may move toward groundwater more readily in organic-rich soils, potentially impacting groundwater quality.

Wang et al. (2013a,b) conducted research on BCNPs mobility in soil with BCNPs produced from wheat straw at two pyrolysis temperature levels (350°C and 500°C). The impacts of various environmentally relevant concentrations of humic acid (HA, 0, 1, 5, and 10 mg/L) and fractional surface coverages of iron oxyhydroxide coatings on sand grains ( $\omega$ , 0.00, 0.16, 0.28, and 0.40) were tested. The study confirmed that BCNP mobility increased linearly with the increase of HA concentration because of electrostatic repulsion between BCNPs and sand grains with adsorbed humic acids. In contrast, the transport of BCNPs significantly decreased with the rise of  $\omega$ , because of the electrostatic interaction between the negative net charge of BCNPs and positively charged surfaces of iron oxyhydroxides. BCNPs transport in the soil environment depends on numerous competitive factors such as the presence of natural organic matter and metal oxide grain coatings.

Other studies on the BCNPs have shown a range of impacts of BCNPs on plant germination and growth when applied to soils and water. (Yue et al., 2019) studied the impact of BCNPs on rice plant growth, applying rice-hull BCNPs that were carbonized at various temperatures (300°C, 400°C, 500°C, and 600°C) in the absence of oxygen. The research divided rice plant growth parameters into several indicators, such as plant height, dry weight, and root morphology. The rice plants with BCNPs amended into the media (produced at pyrolysis temperatures of 400°C and 500°C) had significantly higher biomass dry weight (shoots and roots) than those without BCNPs. The root vitality of rice plants was also increased by the presence of BCNPs, in the order of: control (no BCNPs) < BCNPs (300°C) < BCNPs (400°C) < BCNPs (500°C)  $\approx$  BCNPs (600°C). It was also observed that BCNPs could induce oxidative stress in rice plants, as the presence of higher-temperature BCNPs promotes antioxidative enzyme activities [e.g., superoxide dismutase (SOD), peroxidase (POD), and catalase (CAT) and soluble protein]. High pyrolysis temperature results in BCNPs that have greater pore structures and higher Si content, yielding higher surface reactivity. This is important because BCNPs may have attached to and formed a shell-like structure on root surfaces of rice, which significantly inhibits metal(loid)s absorption by plant, reducing toxicity in contaminated soils.

Zhang et al. (2020) studied the seed germination and growth of rice (*Oryza sativa*), tomato (*Lycopersicon esculentum*), and reed (*Phragmites australis*) seedlings in the presence of six types of BCNPs in the growth media. The BCNPs feedstocks were rice straw and wood sawdust pyrolyzed at 300°C (low), 500°C (mid), and 600°C (high). The results show that BCNPs produced at high pyrolysis temperature inhibited seed germination of rice. Nevertheless, all the rice plant treatments show that BCNPs promote significant increases in root and shoot length. In contrast, high temperature BCNPs inhibited reed growth, evidenced by decreased shoot length and plant biomass. However, no evidence was found that BCNPs affect the tomato plant germination or the growth of seedlings. Cumulatively, these results show that matching an appropriate BCNP to particular plant types, and considering soil and porewater chemistry, is critical to enhancing plant growth.

## 12.2.2.2 Biochar nanoparticles and contaminant interactions

### 12.2.2.2.1 Pharmaceuticals

The use of various pharmaceutical and hormonal drugs has resulted in contaminant residues in aqueous systems. Due to antibiotics resistance and the resulting risk to human health, antibiotics are categorized as high-risk contaminants in the environment. Yang et al. (2020a,b) experimented with the removal of sulfamethazine (SMT) in quartz sand by BCNPs at three pH levels: 5, 7, and 10. Wheat straw was pyrolyzed at 300°C or 600°C to produce bulk biochar, and subsequently ground to produce BCNPs less than 1  $\mu$ m in size. The adsorption of SMT by BCNP and the zeta potential of BCNPs were measured at the three pH levels. The results showed that, in the presence of SMT, the mobility of BCNPs was reduced at acidic or neutral conditions, while at alkaline conditions, it was increased (increasing electrostatic

repulsion between BCNPs and sand grains). The study shows that the application of BCNPs for antibiotics remediation will be more effective in acidic and neutral soil conditions.

Dong et al. (2018) investigated the removal of 17 $\beta$ -estradiol (E2) from aqueous solution using BCNPs. BCNPs were produced by the slow pyrolysis of bagasse, a dry, pulpy, and fibrous material that is a residue of crushing sugarcane or sorghum stalks during the juice extraction process, at temperatures of 400°C, 600°C, and 800°C (Mag-BCNP400, Mag-BCNP600, and Mag-BCNP800). Mag-BCNPs are advantageous for remediation in that they can be quickly separated from solution using magnetic force and regenerated by ozonation. The resulting composites have surface areas almost 14.5 times higher than have microparticulate biochar, resulting in increased adsorption capacity of biochar. Hydrophobic interactions and  $\pi$ - $\pi$  electron donor-acceptor, both, contribute to E2 adsorption, although the primary mechanism is proposed to shift from hydrophobic interactions to  $\pi$ - $\pi$  interactions with increasing Mag-BCNPs pyrolysis temperature. The study shows that Mag-BCNPs show a promise for the removal of E2 and other pharmaceutical compounds from water.

#### 12.2.2.2.2 Metals and metalloids

Safari et al. (2019) used BCNPs derived from mixed WC pyrolyzed at 500°C to remove copper (Cu) from the aqueous solution. The toxicity of BCNPs toward the planktonic crustacean *Daphnia magna* was tested via a 48 h exposure at BCNP concentrations of 0–80 ppm. The data show that BCNPs without Cu pose no acute toxicity risk to *D. magna* in the tested concentration range. Cu removal by BCNPs was also studied through sorption isotherm experiments conducted at pH 3, 5, and 8. BCNP-Cu binding is rapid, as proved by the rapid centrifugation and separation of the BCNPs after mixing them with the Cu solution. The colloidal stability of the BCNPs combined with an abundance of carboxyl and hydroxyl groups that can scavenge Cu ions explains this experimental result. The sorption data show that BCNPs absorb as much as 22 mg/g in a solution initially containing sub-ppm copper concentrations.

BCNPs have applications in reducing phytotoxicity which is the toxic effect expressed by plants in the presence of contaminants in their environment. Plant seed germination delays and inhibition of plant growth are common indicators of contaminant-induced phytotoxicity (Dias, 2012). Liu et al. (2020) studied the application of BCNPs on reducing the phytotoxicity of Cd toward several plant types in soil. The study tested BCNPs produced from wheat straw feedstock that was pyrolyzed at temperature range varying between 350°C and 550°C. Phytotoxicity tests were conducted in Petri dish experiments that employed four different vegetable seeds: tomato, carrot, lettuce, and cucumber, with Cd concentrations of 0, 50, 80, 100, 120 and 150 mg/L and BCNP concentrations of 0, 50, 100, 150, 200, 300 and 500 mg/L. The pot-groups of experiments were conducted using soil and Chinese cabbage in the presence of 0%, 0.2%, 0.5%, and 1% (wt/wt) BCNPs. At the end of the pot experiment, microbial community analyses were conducted using high-throughput sequencing. The petri dish experiments showed that the germination height and weight of four vegetables plants were dramatically decreased in soil samples that did not contain BCNPs ( $p < 0.05$ ). The use of BCNPs resulted in germination rates that increased linearly with higher concentration of BCNPs. The results suggest that BCNP can improve the decreased germination caused by Cd contamination. In pot experiments, the aqueous Cd concentration was lower in the presence of BCNPs in both the soil and planted Chinese cabbage, *Brassica Chinensis L.*, than in other seed treatments without BCNPs ( $p < 0.05$ ). The addition of BCNPs to the soil samples increased the microbial biomass, microorganism abundance, and diversity of Actinobacteria and Bacteroidetes in Cd-contaminated soil, but reduced the variety of Proteobacteria. The study confirmed that the presence of BCNPs is potentially beneficial for metals-contaminated soils. Nevertheless, further study on BCNPs-metal interactions and its consequences on the viability and metabolism of microorganisms remains a research gap.

#### 12.2.2.2.3 Organic pollutants

BCNPs also show promise in the remediation of organic pollutants. For example, Yang et al. (2017) investigated the transport and retention of BCNPs through saturated porous media in the presence of naphthalene. The research aimed to describe the behavior of BCNPs when introduced as a remedial agent for organic pollutant removal from the environment. The BCNPs were generated from a wheat straw feedstock pyrolyzed at 600°C. They were flowed through saturated quartz sand of 425–600  $\mu$ m in diameter which had been pretreated to remove organic matter and oxides from the sand surface. The experiments tested several pH levels (5, 7.1, and 10) and IS (1, 10, 50 mM NaCl). The naphthalene adsorption data suggest that pH and IS have no impact on the adsorption process. This is explained by the fact that naphthalene is a hydrophobic compound in which the interaction between BCNPs and naphthalene was related to hydrophobic interactions. Analysis of the surface properties of the BCNPs and sand shows that naphthalene shielded a part of the BCNP surface charge due to hydrophobic interactions during adsorption. This charge-shielding caused a

decline in the absolute value of the BCNPs zeta potential. IS also impacted the mobility of BCNPs in the column experiments; namely, transport is impeded as the IS of the aqueous solution increases, while the mobility of BCNPs was slightly lower in the presence of naphthalene for all IS treatments. Finally, the mobility of BCNPs decreased in acidic conditions, while remaining similar at neutral and alkaline conditions. Nevertheless, the IS and pH of soil solution are essential factors in the mobility of BCNPs, which directly impacts the mobility of naphthalene bound to these particles.

## 12.3 Interaction of microorganisms with BCNPs during remediation processes

The application of biochar in the environment requires the consideration of several factors such as the presence of volatile organic compounds (VOCs), minerals, and the generation of free radicals (Spokas et al., 2011). These components may lead to shifts in microbial activity, microbial community structure, as well as biogeochemical processes such as elemental cycling and the organic matter composition of water and soils through changes in enzymatic activity (Paz-Ferreiro et al., 2014).

Various positive reports of the use of biochar and microbes in bioremediation processes have proved that biochar is an effective agent for water and soil bioremediation (Chen and Ding, 2012; Chen et al., 2012; García-Delgado et al., 2015). However, the interactions of BCNPs with microbes and the mechanisms of contaminant degradation or immobilization remain understudied. Microorganisms have the ability to generate PFR and to control electron transfer processes that are essential to the success of biochar-microbe catalyzed remediation. PFRs are formed on biochar during the thermal decomposition process of the feedstock and can subsequently trigger the generation of ROS (Klüpfel et al., 2014; Fang et al., 2015a,b; Yu et al., 2015). Direct electron transfer to organic pollutants can also lead to their degradation or the reductive immobilization of some redox-active metals (Dong et al., 2014; Yu et al., 2015; Yang et al., 2016; Rajapaksha et al., 2018). In addition, the enzymatic reduction of metal(loid)s such as Cr(VI) to Cr(III) is a fundamental process to reduce the toxicity of Cr(VI) toward microbes (Rahman and Thomas, 2021). Oxidoreductase groups—chromosome or plasmid-encoded nonspecific enzymes—primarily catalyze Cr(VI) reduction. These groups contain chromate reductase, NADH-dependent nitroreductase, iron reductase, quinone reductase, and hydrogenases (Pradhan et al., 2016; Baldiris et al., 2018).

BCNPs also contribute to soil decomposition of organic matter as they take part both in the direct extracellular electron transfer (DEET) between soil organic matter (or soil minerals) and microbial cells, and, in the direct interspecific electron transfer (DIET) between microbes (Chen et al., 2014; Fang et al., 2014). Further investigation of the reactive components of biochar particles that regulate electron transfer between BCNPs and microbes is crucial to understand the impacts of biochar on elemental cycling in the environment. BCNPs, as part of bulk biochar, may affect microbial activity through various direct and indirect mechanisms: (1) while BCNPs can induce potential toxicity due to the presence of VOCs and the generation of environmentally PFR (Spokas et al., 2011; Ennis et al., 2012; Fang et al., 2014), and although VOCs may present risks to soils and aquatic environments, VOCs are still a carbon source for the microbes (e.g., *Bacillus mucilaginosus*; Sun et al., 2015); (2) BCNPs modify their surrounding environment by improving soil and water properties essential to crop growth or soil reclamation (Quilliam et al., 2013) such as pH and water content, that can be beneficial for microorganism growth; (3) BCNPs trigger enzyme activity that induces microbially-mediated elemental cycling (Lehmann et al., 2011; Yang et al., 2016); and (4) BCNPs disturb microbial intra- and interspecific cell communication mechanism by a combination of sorption and the hydrolysis of signaling molecules (Masiello et al., 2013; Gao et al., 2016). The complexity of these interactions makes assessing the impacts BCNPs generate on microbial activity during and after biochar application challenging.

### 12.3.1 Surface interactions between BCNPs and microbes

The essential difference between gram-positive bacteria and gram-negative bacteria is the structure of peptidoglycan on their cell wall. Peptidoglycan, the gram-positive bacteria's cell wall, is relatively thick (30%–90% on *Bacillus subtilis*) (Konhauser, 2007) and located outside of the plasma membrane. Peptidoglycan is the interface between external aqueous solution and the surface of bacterial cells. Conversely, gram-negative bacteria have a thinner peptidoglycan layer (10% of the cell wall on *Escherichia coli*; Konhauser, 2007); however, there is a second outer membrane within the cellular envelope. The outer membrane is a porous structure, highly permeable, and dominated by both proteins and lipopolysaccharides (LPS). Both types of bacteria develop extracellular polymeric substance (EPS) that can bind metals, construct minerals, and act as a buffer for chemical substances at the cell periphery, where essential ions accumulate and toxic substances are immobilized. Bacterial EPS serves as a defense mechanism against metal(loid)s toxicity in the

environment. The sheaths function in mediating physiochemical reactions between the inner cell and ions/solids in the external environment. S-layers have the same filtering function that allows for 2–3 nm particles in diameter to enter into and metabolic residues to exit from the cell.

Several functional groups associated with the cell surface, such as hydroxyl, carboxyl, sulfhydryl, and phosphoryl, lead to the formation of an organic anion or ligand and the release of  $H^+$  to the environment. The functional group identities and densities at the surface of microorganisms contribute to the electrical potential of the cell surface and to the spatial distribution of ions at the cell surface (Konhauser, 2007). To provide a comprehensive insight into bacterial surface interactions with BCNPs, surface complexation models (SCM) can be used. Microbial interactions with surfaces of BCNPs are often modeled using the Derjaguin-Landau-Verwey-Overbeek (DLVO) theory that depicts the magnitude and diversity of potential energy at surfaces as a function of separation distance, and predicts particle interactions based on these energies (Fröhlich, 2012). The theory is based in equilibrium thermodynamics, where the Gibbs free energy is minimized by satisfying the charges of the surfaces, which may include those of bacteria (Fig. 12.3).

BCNPs are negatively charged at their intrinsic pH as the result of the deprotonation of oxygen-containing functional groups. The zeta potential of BCNPs is less negative than that of bulk biochar, meaning BCNPs are less stable in the aqueous solution (Song et al., 2019). In addition, pH and solution IS play essential roles in the attachment behavior of BCNPs to microbes. Generally, higher pH or IS result in greater aggregation of BCNPs and microorganisms due to cation bridging effects that cause the two to flocculate (Liu et al., 2017; Yongabi et al., 2021; Marangon et al., 2022).

In the absence of a solid shear force, a bacterium held closely to a mineral surface is ideal for permanent attachment by EPS that physically mediate the interactions between the cell and the solid interface. During starvation, bacteria tend to produce more EPS to trap organic and inorganic substances from the environment. In aqueous environments, BCNPs may be coated with EPS which will impact their dispersion. There are abiotic consequences of this process. BCNPs can decompose releasing component ions and resulting in cellular uptake and toxicity. The accumulation of BCNPs inside the cell may lead to DNA damage, trigger ROS accumulation, and result in associated intracellular damage (Cooper and Goldenberg, 1987; Yeung et al., 2008; Nel et al., 2009; Albanese et al., 2012; Esmailzadeh et al., 2016).

### 12.3.2 Influence of BCNPs on microbial carbon and nutrient cycling

BCNPs may impact nutrient and carbon cycling in water, soil, and aquifers. For example, the use of an  $Fe_3O_4$ -BCNP nanocomposite was reported to significantly increase the removal of chemical oxygen demand (COD) by PSB in

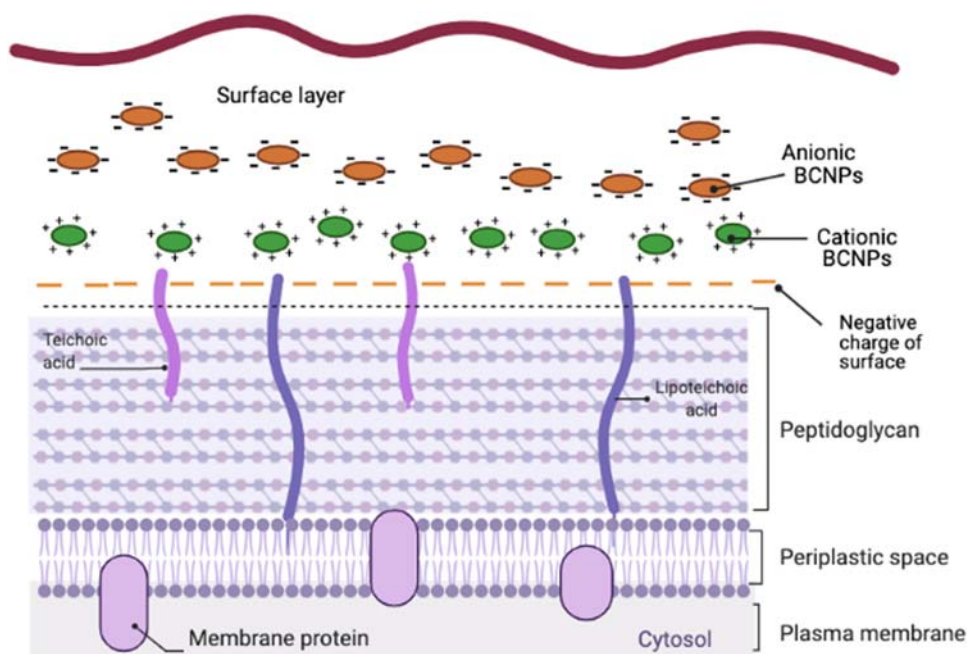


**FIGURE 12.3** Surface properties of gram-positive bacteria and their interactions with BCNPs. Created in Biorender.com.

constructed wetland within the first 30 h of treatment (83% reduction) as compared to the COD removal without the composite material (~65%) (Wang et al., 2016a,b). He et al. (2010), using similar nanocomposites, reported that the presence of nanocomposites increased bacteria bioactivity and metabolism due to the composites' high surface area and nanosize. In this study, the nanocomposite accelerated the removal of  $\text{PO}_4^{3-}$ , removing 92% of the initial contaminant within 20 min of treatment. The high surface area of BCNPs and reactive hydroxide groups were cited as the most plausible mechanisms driving the removal efficiency. In addition, BCNPs provide an additional carbon source for microorganisms, and may provide a sole source of carbon for microbes attached to BCNPs (Liu et al., 2020). Furthermore, during attachment, microbes can release  $\text{H}^+$  to the environment, change the pH of the external environment, and thereby impact nutrient and mineral cycling (Song et al., 2019).

### 12.3.3 Toxicity of BCNPs toward microorganisms

The cytotoxicity of BCNPs toward microorganisms is poorly understood. However, studies that have investigated the interactions of engineered carbonaceous nanoparticles with microbial cells provide a starting point to investigate the toxicity of BCNPs. Like nanoparticles in general, BCNPs are potentially harmful to the microbes as BCNPs have strong affinity for heavy metals and other chemicals in the aqueous system (Jiang et al., 2009a,b; Albanese et al., 2012; Esmailzadeh et al., 2016; Wang et al., 2016a,b; Ahmad et al., 2017).

Fig. 12.4 depicts microbial responses to BCNPs from the molecular to community levels. There are two possible ways in which BCNPs can be introduced to the cytoplasm: (1) by membrane disruption, and (2) by cell mediatory organelles that regulate ion exchange between internal and external cell environments. With sorption to cell envelopes, nanoparticles may react with membranes causing physical damage such as has been documented with the piercing of membranes by carbon nanotubes (CNTs) (Ge et al., 2016). Furthermore, intracellular BCNPs or decomposition products of BCNPs may be expelled from the cell. Intact nanoparticles uptake into cells has been observed and may lead to photocatalytic (light-induced) ROS formation, leading to localized membrane damage where nanoparticles are sorbed at membrane receptors following passive cell entry. However, ROS formation, membrane damage, and nanoparticle entry into cells can also occur in the absence of photocatalysis (Pan et al., 2009; Lushchak, 2011; Khanna et al., 2015; Quinteros et al., 2016; Ezraty et al., 2017). Bacterial toxicology of an agent such as BCNPs is often determined using

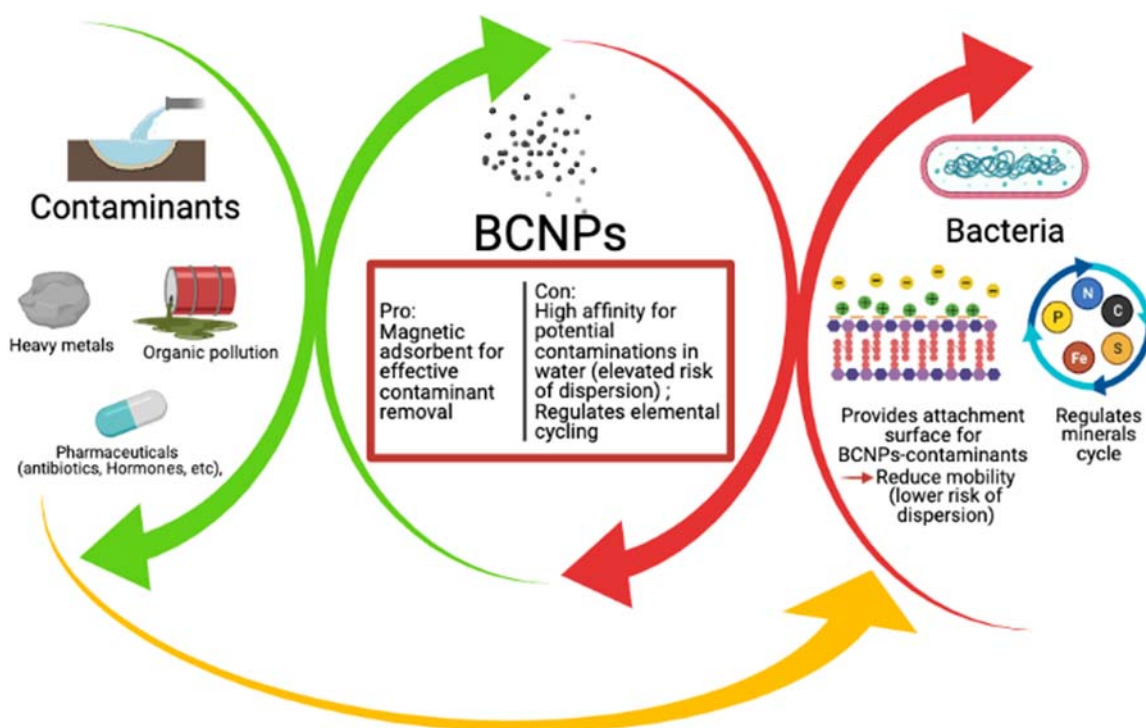


**FIGURE 12.4** Pathways for BCNPs to be introduced into microbial cells. The arrow shows the stages of possible toxicity levels (molecular to the community level). Created in Biorender.com.

the Kirby-Bauer inhibitory zone method. The method is performed in several ways; however, in general, the toxicant is tested by dropping some amount of the agent into the center of an agar plate (or using a filter disk) on which bacteria have been grown. The plate is then incubated, and the transparent area is measured as the growth inhibition afterwards. However, applying this method to test a potential inhibitory agent to bacterial growth inherently tests a broad range of responses (Hudzicki, 2012; Lewis et al., 2019).

Many studies of common nanoparticle toxicity toward bacteria have been conducted, and the response to particular toxicants is often related to the types of bacteria within a species (strain level) (Ruparelia et al., 2008; Dinesh et al., 2012; Maurer-Jones et al., 2013). For instance, *B. subtilis* MTCC 441 has a minimum inhibitory concentration (MIC) of silver nanoparticles of 0.37, similar to *E. coli* MTCC 443, while *E. coli* MTCC 739 and MTCC 1302 had MICs of 1.67 mM and 1.11 mM, respectively (Ruparelia et al., 2008). The responses of both gram-positive and gram-negative bacteria toward nanoparticles has been tested. For example, Feng et al. (2000) found that *Staphylococcus aureus* (a gram-positive bacterium) was more resistant to morphological changes induced by silver nanoparticles than was *E. coli* (gram-negative). However, another study showed that *B. subtilis* has greater sensitivity to nanoparticles (silver and copper) than *E. coli*, as the concentration where survival equals 10% (or C90) of *B. subtilis* was 297  $\mu\text{M}$  while it was 541.2  $\mu\text{M}$  for *E. coli*. The impacts on bacteria of the presence of common solution ions (e.g.,  $\text{Ca}^{2+}$ ,  $\text{Mg}^{2+}$ ,  $\text{Na}^+$ ,  $\text{K}^+$ ,  $\text{SO}_4^{2-}$ ,  $\text{HCO}_3^-$ ) were observed for the antimicrobial experiments where *B. subtilis* and *P. putida* were cultured in the presence of silver nanoparticles, with *P. putida* being more tolerant than was *B. subtilis*. Solution chemistry impacted the bacterial physiology and nanoparticle behavior and, ultimately, impacted the presence of nanoparticles into increasing the microbial toxicity response (Yoon et al., 2007).

Studies of nanoparticle behavior toward bacteria have proved that nanoparticles attach and can also cause competition with other ions to bind to the bacterial surface (Gorman-Lewis et al., 2005; Jiang et al., 2009a,b; Albanese et al., 2012). Attachment can cause fragmentation in peptidoglycan strands, triggering compromised cell walls and/or membrane disruption (Priester et al., 2009; Mirzajani et al., 2011). Lewis et al. (2017) reported evidence of increased  $\text{O}_2$  consumption and viability of *Bacillus amyloliquefaciens* and *P. putida* in the presence of silver nanoparticles, but *S. Meliloti* exhibited a reduction in  $\text{O}_2$  consumption.

Transcriptomic studies on *E. coli* show evidence for differing gene expression patterns upon exposure to nanoparticles (Ivask et al., 2014; Mcquillan and Shaw, 2014). For example, Gambino et al. (2015) observed the inhibition of *B. subtilis* growth and reduced generation time of *Azotobacter vinelandii* in response to the presence of silver nanoparticles in the growth media; however, membrane damage was not reported. Bacterial intra/extracellular ROS levels were also measured and were found to be reduced or unaltered by nanoparticles in *B. subtilis* biofilms. The same research analyzed total protein levels. They were found to be reduced by  $\sim 43\%$  after 2–3 days of biofilm culturing in the 93  $\mu\text{M}$  Ag-nanoparticles treatment, while the 9.3  $\mu\text{M}$  treatment showed a 41% increase in protein at day 4. However, after 5 days, both treatments markedly increase the production of EPS, by approximately 300%, but with no significant shifts in the concentration of environmental DNA (eDNA, or DNA released from the cells) or total protein. The authors also report upregulation of proteins from Gene Ontology (GO) analysis of *B. subtilis* biofilms. Protein is a fundamental substance as it is responsible for primary metabolism, transcription, translation, and quorum sensing. Therefore analysis of stress response proteins is essential to describe and predict further stress-responses (oxidative and redox status of the cell). To summarize, further analysis on changes to microbial growth, proteomic levels, and metabolic responses is required to provide a comprehensive understanding of the toxicity of BCNPs toward microbes.

## 12.4 Conclusions

The development and application of BCNPs, whether added directly for water treatment, soil remediation, or to enhance crop growth, or as a by-product of bulk biochar-degradation, are understudied. The unique physicochemical properties of BCNPs pose both advantages and disadvantages in the environment. Due to their high affinity for metal(loid)s and organic compounds, BCNPs show promise as a tool for contaminant removal from soil and water. However, BCNPs can be mobile and this presents a concern of wider-pollutant dispersion beyond the zone of BCNP or bulk biochar application. Unlike generic nanoparticles, interactions between BCNPs and microbes are lacking. This gap could be filled out by further experiments focusing on surface interactions and by applying the genomic approach, using existing methods applied to the study of a range of nanoparticles. The results of such studies will yield a better understanding of how BCNPs affect microorganisms in natural environments, and what impacts those changes have on biogeochemical cycle in the surrounding environment.

## Acknowledgment

Indonesia Endowment Fund for Education, Ministry of Finance of The Republic of Indonesia for a scholarship grant to DCP, and the Natural Sciences and Engineering Research Council of Canada (NSERC) Discovery program (RGPIN-2020–05289 for a research grant to DSA).

## References

- Ahmad, A., et al., 2017. The effects of bacteria-nanoparticles interface on the antibacterial activity of green synthesized silver nanoparticles. *Microb. Pathogenesis* 102, 133–142. Available from: <https://doi.org/10.1016/j.micpath.2016.11.030>.
- Ahmad, M., Rajapaksha, A.U., Lim, J.E., et al., 2014. Biochar as a sorbent for contaminant management in soil and water: A review. *Chemosphere* 99, 19–33. Available from: <https://doi.org/10.1016/j.chemosphere.2013.10.071>.
- Albanese, A., Tang, P.S., Chan, W.C.W., 2012. The effect of nanoparticle size, shape, and surface chemistry on biological systems. *Annu. Rev. Biomed. Eng.* 14, 1–16. Available from: <https://doi.org/10.1146/annurev-bioeng-071811-150124>.
- Amini, E., et al., 2019. Characterization of pyrolysis products from slow pyrolysis of live and dead vegetation native to the southern United States. *Fuel* 235 (September 2018), 1475–1491. Available from: <https://doi.org/10.1016/j.fuel.2018.08.112>.
- Baldiris, R., et al., 2018. Reduction of hexavalent chromium and detection of chromate reductase (ChrR) in *Stenotrophomonas maltophilia*. *Molecules*. Available from: <https://doi.org/10.3390/molecules23020406>.
- Cao, X., Harris, W., 2010. Properties of dairy-manure-derived biochar pertinent to its potential use in remediation. *Bioresour. Technol.* 101 (14), 5222–5228. Available from: <https://doi.org/10.1016/j.biortech.2010.02.052>.
- Chen, B., Ding, J., 2012. Biosorption and biodegradation of phenanthrene and pyrene in sterilized and unsterilized soil slurry systems stimulated by *Phanerochaete chrysosporium*. *J. Hazard. Mater.* 229–230, 159–169. Available from: <https://doi.org/10.1016/j.jhazmat.2012.05.090>.
- Chen, B., Zhou, D., Zhu, L., 2008. Transitional adsorption and partition of nonpolar and polar aromatic contaminants by biochars of pine needles with different pyrolytic temperatures. *Environ. Sci. Technol.* Available from: <https://doi.org/10.1021/es8002684>.
- Chen, B., Yuan, M., Qian, L., 2012. Enhanced bioremediation of PAH-contaminated soil by immobilized bacteria with plant residue and biochar as carriers. *J. Soils Sediment.* 12 (9), 1350–1359. Available from: <https://doi.org/10.1007/s11368-012-0554-5>.
- Chen, S., et al., 2014. Promoting interspecies electron transfer with biochar. *Sci. Rep.* 4. Available from: <https://doi.org/10.1038/srep05019>.
- Chen, M., et al., 2017. Transport and retention of biochar nanoparticles in a paddy soil under environmentally-relevant solution chemistry conditions. *Environ. Pollut.* Available from: <https://doi.org/10.1016/j.envpol.2017.06.101>.
- Conti, R., et al., 2014. Evaluation of the thermal and environmental stability of switchgrass biochars by Py-GC-MS. *J. Anal. Appl. Pyrolysis* 110 (1), 239–247. Available from: <https://doi.org/10.1016/j.jaap.2014.09.010>.
- Cooper, D.G., Goldenberg, B.G., 1987. Surface-active agents from two *Bacillus* species. *Appl. Environ. Microbiol.* 53 (2), 224–229. Available from: <https://doi.org/10.1128/aem.53.2.224-229.1987>.
- Dias, M.C., 2012. Phytotoxicity: an overview of the physiological responses of plants exposed to fungicides. *J. Botany* 2012, 1–4. Available from: <https://doi.org/10.1155/2012/135479>.
- Dinesh, R., et al., 2012. Engineered nanoparticles in the soil and their potential implications to microbial activity. *Geoderma*. Available from: <https://doi.org/10.1016/j.geoderma.2011.12.018>.
- Dong, X., et al., 2014. Enhanced Cr(VI) reduction and As(III) oxidation in ice phase: important role of dissolved organic matter from biochar. *J. Hazard. Mater.* Available from: <https://doi.org/10.1016/j.jhazmat.2013.12.027>.
- Dong, X., et al., 2018. Removal of 17 $\beta$ -estradiol by using highly adsorptive magnetic biochar nanoparticles from aqueous solution. *Chem. Eng. J.* 352 (July), 371–379. Available from: <https://doi.org/10.1016/j.cej.2018.07.025>.
- Downie, A., Crosky, A., Munroe, P., 2012. Physical properties of biochar. In: *Biochar for Environmental Management: Science and Technology*. Taylor and Francis. Available from: <https://doi.org/10.4324/9781849770552>.
- Ennis, C.J., et al., 2012. Biochar: carbon sequestration, land remediation, and impacts on soil microbiology. *Crit. Rev. Environ. Sci. Technol.* 42 (22), 2311–2364. Available from: <https://doi.org/10.1080/10643389.2011.574115>.
- Esmailzadeh, H., et al., 2016. Effect of nanocomposite packaging containing ZnO on growth of *Bacillus subtilis* and *Enterobacter aerogenes*. *Mater. Sci. Eng. C.* 58, 1058–1063. Available from: <https://doi.org/10.1016/j.msec.2015.09.078>.
- Ezraty, B., et al., 2017. Oxidative stress, protein damage and repair in bacteria. *Nat. Rev. Microbiol.* Available from: <https://doi.org/10.1038/nrmicro.2017.26>.
- Fang, G., et al., 2014. Key role of persistent free radicals in hydrogen peroxide activation by biochar: Implications to organic contaminant degradation. *Environ. Sci. Technol.* 48 (3), 1902–1910. Available from: <https://doi.org/10.1021/es4048126>.
- Fang, G., Liu, C., et al., 2015a. Manipulation of persistent free radicals in biochar to activate persulfate for contaminant degradation. *Environ. Sci. Technol.* Available from: <https://doi.org/10.1021/es5061512>.
- Fang, G., Zhu, C., et al., 2015b. Mechanism of hydroxyl radical generation from biochar suspensions: implications to diethyl phthalate degradation. *Bioresour. Technol.* Available from: <https://doi.org/10.1016/j.biortech.2014.11.032>.
- Feng, Q.L., et al., 2000. A mechanistic study of the antibacterial effect of silver ions on *Escherichia coli* and *Staphylococcus aureus*. *J. Biomed. Mater. Res.* 52 (4), 662–668. Available from: [https://doi.org/10.1002/1097-4636\(20001215\)52:4 < 662::AID-JBM10 > 3.0.CO;2-3](https://doi.org/10.1002/1097-4636(20001215)52:4 < 662::AID-JBM10 > 3.0.CO;2-3).
- Fröhlich, E., 2012. The role of surface charge in cellular uptake and cytotoxicity of medical nanoparticles. *Int. J. Nanomed.* 7, 5577–5591. Available from: <https://doi.org/10.2147/IJN.S36111>.

- Fu, P., et al., 2011. Effect of temperature on gas composition and char structural features of pyrolyzed agricultural residues. *Bioresour. Technol.* Available from: <https://doi.org/10.1016/j.biortech.2011.05.083>.
- Gambino, M., et al., 2015. Effects of sublethal doses of silver nanoparticles on *Bacillus subtilis* planktonic and sessile cells. *J. Appl. Microbiol.* 118 (5), 1103–1115. Available from: <https://doi.org/10.1111/jam.12779>.
- Gao, X., et al., 2016. Charcoal disrupts soil microbial communication through a combination of signal sorption and hydrolysis. *ACS Omega* 1 (2), 226–233. Available from: <https://doi.org/10.1021/acsomega.6b00085>.
- García-Delgado, C., Alfaro-Barta, I., Eymar, E., 2015. Combination of biochar amendment and mycoremediation for polycyclic aromatic hydrocarbons immobilization and biodegradation in creosote-contaminated soil. *J. Hazard. Mater.* 285, 259–266. Available from: <https://doi.org/10.1016/j.jhazmat.2014.12.002>.
- Ge, Y., et al., 2016. Long-term effects of multiwalled carbon nanotubes and graphene on microbial communities in dry soil. *Environ. Sci. Technol.* 50 (7), 3965–3974. Available from: <https://doi.org/10.1021/acs.est.5b05620>.
- Gorman-Lewis, D., et al., 2005. Experimental study of neptunyl adsorption onto *Bacillus subtilis*. *Geochim. Cosmochim. Acta* 69 (20), 4837–4844. Available from: <https://doi.org/10.1016/j.gca.2005.06.028>.
- Guo, S.s., et al., 2019. Properties of ball-milled biochar and its toxic effects on *E.coli* and *S. aureus*. *J. Agro-Environ. Sci.* Available from: <https://doi.org/10.11654/jaes.2018-1617>.
- Hale, S.E., et al., 2012. Quantifying the total and bioavailable polycyclic aromatic hydrocarbons and dioxins in biochars. *Environ. Sci. Technol.* Available from: <https://doi.org/10.1021/es203984k>.
- He, C., et al., 2010. Effects of particle size and surface charge on cellular uptake and biodistribution of polymeric nanoparticles. *Biomaterials* 31 (13), 3657–3666. Available from: <https://doi.org/10.1016/j.biomaterials.2010.01.065>.
- He, S., et al., 2016. Different responses of soil microbial metabolic activity to silver and iron oxide nanoparticles. *Chemosphere*. Available from: <https://doi.org/10.1016/j.chemosphere.2015.12.055>.
- Hudzicki, J., 2012. Kirby-Bauer disk diffusion susceptibility test protocol author information. *Am. Soc. For. Microbiol.* 1–13 (December 2009) Available at. Available from: <https://www.asm.org/Protocols/Kirby-Bauer-Disk-Diffusion-Susceptibility-Test-Pro>.
- Ivask, A., et al., 2014. Toxicity mechanisms in *Escherichia coli* vary for silver nanoparticles and differ from ionic silver. *ACS Nano* 8 (1), 374–386. Available from: <https://doi.org/10.1021/nn4044047>.
- Jaisi, D.P., Elimelech, M., 2009. Single-walled carbon nanotubes exhibit limited transport in soil columns. *Environ. Sci. Technol.* 43 (24), 9161–9166. Available from: <https://doi.org/10.1021/es901927y>.
- Jiang, J., Oberdörster, G., Biswas, P., 2009a. Characterization of size, surface charge, and agglomeration state of nanoparticle dispersions for toxicological studies. *J. Nanopart. Res.* 11 (1), 77–89. Available from: <https://doi.org/10.1007/s11051-008-9446-4>.
- Jiang, W., Mashayekhi, H., Xing, B., 2009b. Bacterial toxicity comparison between nano- and micro-scaled oxide particles. *Environ. Pollut.* 157 (5), 1619–1625. Available from: <https://doi.org/10.1016/j.envpol.2008.12.025>.
- Jin, J., et al., 2016. Influence of pyrolysis temperature on properties and environmental safety of heavy metals in biochars derived from municipal sewage sludge. *J. Hazard. Mater.* Available from: <https://doi.org/10.1016/j.jhazmat.2016.08.050>.
- Jouhara, H., et al., 2018. Pyrolysis of domestic based feedstock at temperatures up to 300 °C. *Therm. Sci. Eng. Prog.* 5 (October 2017), 117–143. Available from: <https://doi.org/10.1016/j.tsep.2017.11.007>.
- Kalus, K., Koziel, J.A., Opaliński, S., 2019. A review of biochar properties and their utilization in crop agriculture and livestock production. *Appl. Sci. (Switz.)* 9 (17). Available from: <https://doi.org/10.3390/app9173494>.
- Khanna, P., et al., 2015. Nanotoxicity: an interplay of oxidative stress, inflammation and cell death. *Nanomaterials*. Available from: <https://doi.org/10.3390/nano5031163>.
- Kim, Y., et al., 2019. Modification of biochar properties using CO<sub>2</sub>. *Chem. Eng. J.* 372 (April), 383–389. Available from: <https://doi.org/10.1016/j.cej.2019.04.170>.
- Klöpffel, L., et al., 2014. Redox properties of plant biomass-derived black carbon (biochar). *Environ. Sci. Technol.* 48 (10), 5601–5611. Available from: <https://doi.org/10.1021/es500906d>.
- Konhauser, K., 2007. *Introduction to Geomicrobiology*, first ed. Wiley. Available from: <https://www.perlego.com/book/2762478/introduction-to-geomicrobiology-pdf>.
- Lehmann, J., et al., 2011. Biochar effects on soil biota - a review. *Soil Biol. Biochem.* 43 (9), 1812–1836. Available from: <https://doi.org/10.1016/j.soilbio.2011.04.022>.
- Leng, L., et al., 2021. An overview on engineering the surface area and porosity of biochar. *Sci. Total Environ.* 763, 144204. Available from: <https://doi.org/10.1016/j.scitotenv.2020.144204>.
- Lewis, R.W., et al., 2017. Silver engineered nanomaterials and ions elicit species-specific O<sub>2</sub> consumption responses in plant growth promoting rhizobacteria. *Biointerphases* 12 (5), 05G604. Available from: <https://doi.org/10.1116/1.4995605>.
- Lewis, R.W., Bertsch, P.M., McNear, D.H., 2019. Nanotoxicity of engineered nanomaterials (ENMs) to environmentally relevant beneficial soil bacteria—a critical review. *Nanotoxicology* 13 (3), 392–428. Available from: <https://doi.org/10.1080/17435390.2018.1530391>.
- Liu, B., Poolman, B., Boersma, A.J., 2017. Ionic strength sensing in living cells. *ACS Chem. Biol.* 12 (10), 2510–2514. Available from: <https://doi.org/10.1021/acscchembio.7b00348>.
- Liu, G., et al., 2018. Formation and physicochemical characteristics of nano biochar: insight into chemical and colloidal stability. *Environ. Sci. Technol.* 52 (18), 10369–10379. Available from: <https://doi.org/10.1021/acs.est.8b01481>.
- Liu, W., et al., 2020. The effectiveness of nanobiochar for reducing phytotoxicity and improving soil remediation in cadmium-contaminated soil. *Sci. Rep.* 10 (1), 1–10. Available from: <https://doi.org/10.1038/s41598-020-57954-3>.

- Lushchak, V.I., 2011. Adaptive response to oxidative stress: bacteria, fungi, plants and animals. *Comp. Biochem. Physiol. C. Toxicol. Pharmacol.* 153 (2), 175–190. Available from: <https://doi.org/10.1016/j.cbpc.2010.10.004>.
- Marangon, C.A., et al., 2022. The effects of ionic strength and pH on antibacterial activity of hybrid biosurfactant-biopolymer nanoparticles. *J. Appl. Polym. Sci.* Available from: <https://doi.org/10.1002/app.51437>.
- Masiello, C.A., et al., 2013. Biochar and microbial signaling: Production conditions determine effects on microbial communication. *Environ. Sci. Technol.* 47 (20), 11496–11503. Available from: <https://doi.org/10.1021/es401458s>.
- Maurer-Jones, M.A., et al., 2013. Toxicity of engineered nanoparticles in the environment. *Anal. Chem.* 85 (6), 3036–3049. Available from: <https://doi.org/10.1021/ac303636s>.
- McBeath, A.V., et al., 2011. Determination of the aromaticity and the degree of aromatic condensation of a thermosequence of wood charcoal using NMR. *Org. Geochem.* 42 (10), 1194–1202. Available from: <https://doi.org/10.1016/j.orggeochem.2011.08.008>.
- Mcquillan, J.S., Shaw, A.M., 2014. Whole-cell *Escherichia coli*-based bio-sensor assay for dual zinc oxide nanoparticle toxicity mechanisms. *Biosens. Bioelectron.* 51, 274–279. Available from: <https://doi.org/10.1016/j.bios.2013.07.024>.
- Mirzajani, F., et al., 2011. Antibacterial effect of silver nanoparticles on *Staphylococcus aureus*. *Res. Microbiol.* 162 (5), 542–549. Available from: <https://doi.org/10.1016/j.resmic.2011.04.009>.
- Nel, A.E., et al., 2009. Understanding biophysicochemical interactions at the nano-bio interface. *Nat. Mater.* 8 (7), 543–557. Available from: <https://doi.org/10.1038/nmat2442>.
- Nyoka, N.W.K., et al., 2018. Biochar alleviates the toxicity of imidacloprid and silver nanoparticles (AgNPs) to *Enchytraeus albidus* (Oligochaeta). *Environ. Sci. Pollut. Res.* Available from: <https://doi.org/10.1007/s11356-018-1383-x>.
- Oleszczuk, P., et al., 2016. Characterization of nanoparticles of biochars from different biomass. *J. Anal. Appl. Pyrolysis* 121, 165–172. Available from: <https://doi.org/10.1016/j.jaap.2016.07.017>.
- Pan, Y., et al., 2009. Gold nanoparticles of diameter 1.4 nm trigger necrosis by oxidative stress and mitochondrial damage. *Small.* Available from: <https://doi.org/10.1002/smll.200900466>.
- Paz-Ferreiro, J., et al., 2014. Use of phytoremediation and biochar to remediate heavy metal polluted soils: a review. *Solid Earth* 5 (1), 65–75. Available from: <https://doi.org/10.5194/se-5-65-2014>.
- Pradhan, S.K., et al., 2016. Bacterial chromate reduction: a review of important genomic, proteomic, and bioinformatic analysis. *Crit. Rev. Environ. Sci. Technol.* 46 (21–22), 1659–1703. Available from: <https://doi.org/10.1080/10643389.2016.1258912>.
- Priester, J.H., et al., 2009. Effects of soluble cadmium salts vs cdse quantum dots on the growth of planktonic *Pseudomonas aeruginosa*. *Environ. Sci. Technol.* 43 (7), 2589–2594. Available from: <https://doi.org/10.1021/es802806n>.
- Quilliam, R.S., et al., 2013. Life in the “charosphere” - does biochar in agricultural soil provide a significant habitat for microorganisms? *Soil Biol. Biochem.* 65, 287–293. Available from: <https://doi.org/10.1016/j.soilbio.2013.06.004>.
- Quinteros, M.A., et al., 2016. Oxidative stress generation of silver nanoparticles in three bacterial genera and its relationship with the antimicrobial activity. *Toxicol. Vitro.* Available from: <https://doi.org/10.1016/j.tiv.2016.08.007>.
- Rahman, Z., Thomas, L., 2021. Chemical-assisted microbially mediated chromium (Cr) (VI) reduction under the influence of various electron donors, redox mediators, and other additives: an outlook on enhanced Cr(VI) removal. *Front. Microbiol.* 11 (January), 1–19. Available from: <https://doi.org/10.3389/fmicb.2020.619766>.
- Rajapaksha, A.U., Alam, M.S., Chen, N., Alessi, D.S., et al., 2018. Removal of hexavalent chromium in aqueous solutions using biochar: Chemical and spectroscopic investigations. *Sci. Total Environ.* 625, 1567–1573. Available from: <https://doi.org/10.1016/j.scitotenv.2017.12.195>.
- Ruparelia, J.P., et al., 2008. Strain specificity in antimicrobial activity of silver and copper nanoparticles. *Acta Biomater.* 4 (3), 707–716. Available from: <https://doi.org/10.1016/j.actbio.2007.11.006>.
- Safari, S., et al., 2019. Biochar colloids and their use in contaminants removal. *Biochar* 1 (2), 151–162. Available from: <https://doi.org/10.1007/s42773-019-00014-5>.
- Sagee, O., Dror, I., Berkowitz, B., 2012. Transport of silver nanoparticles (AgNPs) in soil. *Chemosphere* 670–675. Available from: <https://doi.org/10.1016/j.chemosphere.2012.03.055>.
- Song, B., et al., 2019. Physicochemical property and colloidal stability of micron- and nano-particle biochar derived from a variety of feedstock sources. *Sci. Total Environ.* 661, 685–695. Available from: <https://doi.org/10.1016/j.scitotenv.2019.01.193>.
- Spokas, K.A., et al., 2011. Qualitative analysis of volatile organic compounds on biochar. *Chemosphere* 85 (5), 869–882. Available from: <https://doi.org/10.1016/j.chemosphere.2011.06.108>.
- Suliman, W., et al., 2017. The role of biochar porosity and surface functionality in augmenting hydrologic properties of a sandy soil. *Sci. Total Environ.* 574 (March 2018), 139–147. Available from: <https://doi.org/10.1016/j.scitotenv.2016.09.025>.
- Sun, D., et al., 2015. Effect of volatile organic compounds absorbed to fresh biochar on survival of *Bacillus mucilaginosus* and structure of soil microbial communities. *J. Soils Sediment.* Available from: <https://doi.org/10.1007/s11368-014-0996-z>.
- Varma, A.K., Mondal, P., 2018. Pyrolysis of pine needles: effects of process parameters on products yield and analysis of products. *J. Therm. Anal. Calorim.* Available from: <https://doi.org/10.1007/s10973-017-6727-0>.
- Vassilev, S.V., et al., 2013. An overview of the composition and application of biomass ash. Part 1. Phase-mineral and chemical composition and classification. *Fuel* 105, 40–76. Available from: <https://doi.org/10.1016/j.fuel.2012.09.041>.
- Wang, Y., et al., 2010. Transport and retention of fullerene nanoparticles in natural soils. *J. Environ. Qual.* Available from: <https://doi.org/10.2134/jeq2009.0411>.

- Wang, D., et al., 2013a. Transport of biochar particles in saturated granular media: effects of pyrolysis temperature and particle size. *Environ. Sci. Technol.* Available from: <https://doi.org/10.1021/es303794d>.
- Wang, D., Zhang, W., Zhou, D., 2013b. Antagonistic effects of humic acid and iron oxyhydroxide grain-coating on biochar nanoparticle transport in saturated sand. *Environ. Sci. Technol.* 47 (10), 5154–5161. Available from: <https://doi.org/10.1021/es305337r>.
- Wang, C., et al., 2016a. Green synthesis of silver nanoparticles by *Bacillus methylophilicus*, and their antimicrobial activity. *Artif. Cells, Nanomed. Biotechnol.* 44 (4), 1127–1132. Available from: <https://doi.org/10.3109/21691401.2015.1011805>.
- Wang, W., et al., 2016b. Treatment of rich ammonia nitrogen wastewater with polyvinyl alcohol immobilized nitrifier biofortified constructed wetlands. *Ecol. Eng.* Available from: <https://doi.org/10.1016/j.ecoleng.2016.05.078>.
- Weber, K., Quicker, P., 2018. Properties of biochar. *Fuel* 217 (December 2017), 240–261. Available from: <https://doi.org/10.1016/j.fuel.2017.12.054>.
- Woods, W.I., et al., 2009. Amazonian dark earths: Wim Sombroek's vision. *Amazonian Dark Earths: Wim Sombroek's Vis.* November, 1–502. Available from: <https://doi.org/10.1007/978-1-4020-9031-8>.
- Xing, Y., et al., 2016. Colloid-mediated transport of pharmaceutical and personal care products through porous media. *Sci. Rep.* 6, 1–10. Available from: <https://doi.org/10.1038/srep35407>.
- Xu, F., et al., 2017. Aggregation behavior of dissolved black carbon: implications for vertical mass flux and fractionation in aquatic systems. *Environ. Sci. Technol.* Available from: <https://doi.org/10.1021/acs.est.7b04232>.
- Yang, H., et al., 2007. Characteristics of hemicellulose, cellulose and lignin pyrolysis. *Fuel* 86 (12–13), 1781–1788. Available from: <https://doi.org/10.1016/j.fuel.2006.12.013>.
- Yang, J., et al., 2016. Degradation of p-nitrophenol on biochars: role of persistent free radicals. *Environ. Sci. Technol.* 50 (2), 694–700. Available from: <https://doi.org/10.1021/acs.est.5b04042>.
- Yang, W., et al., 2017. Effect of naphthalene on transport and retention of biochar colloids through saturated porous media. *Colloids Surf. A: Physicochem. Eng. Asp.* 530 (July), 146–154. Available from: <https://doi.org/10.1016/j.colsurfa.2017.07.010>.
- Yang, W., et al., 2019. Colloidal stability and aggregation kinetics of biochar colloids: effects of pyrolysis temperature, cation type, and humic acid concentrations. *Sci. Total Environ.* Available from: <https://doi.org/10.1016/j.scitotenv.2018.12.269>.
- Yang, W., Feng, T., et al., 2020a. Effect of sulfamethazine on surface characteristics of biochar colloids and its implications for transport in porous media. *Environ. Pollut.* 256. Available from: <https://doi.org/10.1016/j.envpol.2019.113482>.
- Yang, W., Shang, J., et al., 2020b. Surface and colloid properties of biochar and implications for transport in porous media. *Crit. Rev. Environ. Sci. Technol.* 50 (23), 2484–2522. Available from: <https://doi.org/10.1080/10643389.2019.1699381>.
- Yeung, T., et al., 2008. Membrane phosphatidylserine regulates surface charge and protein localization. *Science* 319 (5860), 210–213. Available from: <https://doi.org/10.1126/science.1152066>.
- Yongabi, D., et al., 2021. Ionic strength controls long-term cell-surface interactions – A QCM-D study of *S. cerevisiae* adhesion, retention and detachment. *J. Colloid Interface Sci.* 585, 583–595. Available from: <https://doi.org/10.1016/j.jcis.2020.10.038>.
- Yoon, K.Y., et al., 2007. Susceptibility constants of *Escherichia coli* and *Bacillus subtilis* to silver and copper nanoparticles. *Sci. Total Environ.* 373 (2–3), 572–575. Available from: <https://doi.org/10.1016/j.scitotenv.2006.11.007>.
- Yu, L., et al., 2015. Biochar as an electron shuttle for reductive dechlorination of pentachlorophenol by *Geobacter sulfurreducens*. *Sci. Rep.* Available from: <https://doi.org/10.1038/srep16221>.
- Yuan, J.H., Xu, R.K., Zhang, H., 2011. The forms of alkalis in the biochar produced from crop residues at different temperatures. *Bioresour. Technol.* 102 (3), 3488–3497. Available from: <https://doi.org/10.1016/j.biortech.2010.11.018>.
- Yue, L., et al., 2019. The effect of biochar nanoparticles on rice plant growth and the uptake of heavy metals: implications for agronomic benefits and potential risk. *Sci. Total Environ.* 656, 9–18. Available from: <https://doi.org/10.1016/j.scitotenv.2018.11.364>.
- Zhang, W., et al., 2010. Transport and retention of biochar particles in porous media: effect of pH, ionic strength, and particle size. *Ecohydrology.* Available from: <https://doi.org/10.1002/eco.160>.
- Zhang, K., et al., 2020. Effects of biochar nanoparticles on seed germination and seedling growth. *Environ. Pollut.* 256. Available from: <https://doi.org/10.1016/j.envpol.2019.113409>.
- Zhao, S.X., Ta, N., Wang, X.D., 2017. Effect of temperature on the structural and physicochemical properties of biochar with apple tree branches as feedstock material. *Energies* 10 (9). Available from: <https://doi.org/10.3390/en10091293>.